

## SPATIO-TEMPORAL SCALES OF LAND COVER AND SHORELINE DYNAMICS IN BANAYBANAY, DAVAO ORIENTAL, PHILIPPINES USING AVAILABLE OPTICAL SATELLITE IMAGERY

K. P. Bolanio <sup>1,2</sup>, LG. S. Digal <sup>1</sup>, HJ. R. Estilo <sup>1</sup>, R. A. Seronay <sup>3\*</sup>

<sup>1</sup> Department of Geodetic Engineering, College of Engineering and Geosciences, Caraga State University, Ampayon, Butuan City, 8600, Philippines – (laizagrace.digal, honeyjane.estilo)@carsu.edu.ph  
<sup>2</sup> Caraga Center for Geo-Informatics, Caraga State University, Ampayon, Butuan City, 8600, Philippines – kpbolanio@carsu.edu.ph  
<sup>3</sup> Department of Environmental Sciences, College of Forestry and Environmental Sciences, Caraga State University, Ampayon, Butuan City, 8600, Philippines – romell.seronay@gmail.com

**KEY WORDS:** Land Cover Change, Shoreline Change, Landsat, DSAS, Accretion, Erosion

### ABSTRACT:

Shoreline dynamics are often the most visible indicators of changes that occur in coastal areas. It is essential to consider a shoreline's physical location while evaluating changes on a temporal and chronological scale. The shoreline in Banaybanay, Davao Oriental, has undergone significant land use changes, leading to negative impacts on related coastal processes, including mariculture conditions in the area. This study aims to determine changes in land cover and shoreline in Banaybanay's coastal barangays by analyzing satellite images from 1989-2021 using remote sensing, GIS, and Digital Shoreline Analysis Systems (DSAS). The study found that rapid land cover changes in the area were primarily driven by development growth, urbanization, mining, and human activities. The Net Shoreline Movement (NSM), End Point Rate (EPR), and Linear Regression Rate (LRR) results indicated accretion in Banaybanay's coastal areas, corresponding to an increase in built-ups and barren from 1989-2021. Characterization of land cover and shoreline change revealed high erosion associated with land cover change of barren-water and grassland/brushland-water with a maximum erosion value of -1.19 m/yr. Conversely, very high accretion was mainly characterized by land cover change of water-built-up, barren-built-up, and water-barren with a maximum accretion value of 9.58 m/yr.

### 1. INTRODUCTION

Coastal regions are primarily populated areas of the world. These environmentally delicate zones are under severe strain due to human activities such as urbanization, resource exploitation, pollution, and natural phenomena like climate change (Tamassoki et al., 2014). When assessing changes over time and chronologically, the physical position of a shoreline is a crucial factor to consider. The visualization of shoreline changes through delineation and evaluation of changes over multiple years enhances our understanding of the causes, rates, and impacts of these changes (Azatuhi et al., 2019).

Land use change refers to the conversion of a piece of land into a different type of land, such as cultivated land, grassland, woodland, infrastructure, or residential area. Land cover change (LCC) is an important factor in calculating natural and human-induced changes in land use. LCC is a major driver of environmental change, caused by rapid geomorphological processes such as erosion and accretion, human pressure, and land reclamation initiatives. Changes in coastal land use can directly affect the position of the shoreline, which also shifts due to erosion and accretion. As the use of the coastal area changes, erosion or accretion occurs, altering the shoreline (Islam et al., 2021).

As depicted in Figure 1, the shoreline of Banaybanay, Davao Oriental, has undergone substantial changes in land use, leading to negative impacts on related coastal processes, including the area's mariculture conditions (specifically in terms of maintaining ecological balance). Consequently, it is crucial to evaluate the temporal changes in the shoreline and predict future alterations or the rate of change using remote sensing and

GIS techniques. These methods are effective for detecting, mapping, and monitoring shorelines.



**Figure 1.** Image composite depicting the visual representation of the development that has taken place in barangays Pintatagan and Puntalinao, Banaybanay, Davao Oriental, from 2009 to 2021. Photo credits: Google Earth Pro

The rapid advancement of remote sensing and GIS technology has opened up new possibilities in various fields, including oceanography, particularly in the area of shoreline modification (Thao et al., 2008). Data gathered through remote sensing is invaluable for detecting changes in coastlines and plays a crucial role in data analysis and mapping (Zonkouan et al., 2022). This type of data is extensively used in environmental monitoring programs aimed at tracking changes in surface phenomena over time. Techniques for spatial data analysis and mapping, such as GIS and remote sensing, are commonly used in monitoring environmental and natural resources (Makota et al., 2004).

The primary goal of this research is to evaluate the changes in land cover and shoreline in the coastal barangays of

\* Corresponding author

Banaybanay, Davao Oriental. More specifically, the study seeks to detect changes in land cover in the area using satellite images from 1989-2021, analyze shoreline changes in Banaybanay’s coastal barangays using the Digital Shoreline Analysis System (DSAS), project the shoreline’s position for the next twenty years, and establish a significant correlation between land cover and shoreline kinematics. This research is crucial as it will examine the temporal changes in land cover and shoreline in Banaybanay’s coastal areas. The findings of this study will provide a future projection of the shoreline, which could be instrumental for the local community in managing anthropogenic coastal processes.

## 2. METHODOLOGY

### 2.1 Study Area

This research focuses on the coastal barangays of Banaybanay, Davao Oriental. Banaybanay is a municipality of the second class in Davao Oriental, situated at 7.16°N latitude and 126.16°E longitude in the Davao Region. The municipality encompasses six coastal barangays, namely Maputi, Kalubihan, Mogbongcogon, Piso, Pintatagan, and Puntalinao.

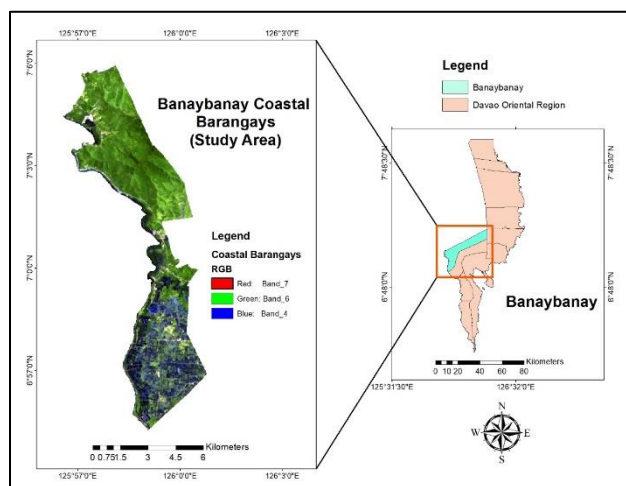


**Figure 2.** The map provides a detailed view of the study area, indicating the location of the coastal barangays within Banaybanay, Davao Oriental, Philippines.

### 2.2 Methodological Framework

The methodological framework of the study, which guides the researcher through the research process, is a critical aspect that requires elucidation to understand the entire procedure. The methodology for this research is bifurcated into two primary processes: detecting changes in land cover and identifying changes in the shoreline.

### 2.3 Datasets

Satellite images for this study were sourced from USGS EarthExplorer. The researchers utilized a series of Landsat images, specifically Landsat TM and Landsat 8 OLI images from the years 1989, 1996, 2017, and 2021. For the years 1989 and 1996, Landsat 5 Thematic Mapper (TM) images were downloaded under collection 2 level 2 from USGS. For the years 2017 and 2021, Landsat 8 Operational Land Imager (OLI) images were used. The two Landsat 8 satellite images obtained underwent a process of radiometric calibration, which involved converting DN values to Top-of-Atmosphere (TOA) Reflectance and were corrected for atmospheric reflectance

using the Dark Object Subtraction Method. All the satellite images obtained were used to identify changes in land cover and shoreline in the area.

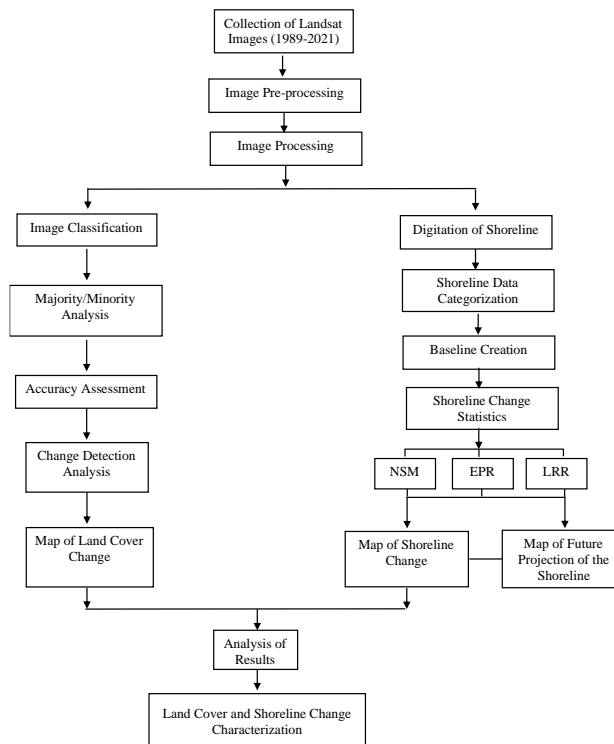


**Figure 3.** This diagram illustrates the methodological framework used in the study of land cover and shoreline changes.

### 2.4 Satellite Image Pre-processing and Classification

Pre-processing is a crucial step when working with raw image datasets, such as Landsat images. This process enhances the efficiency of data representation for further visual interpretation, converting raw data into significant information. The application of image pre-processing transforms primary image datasets into accurately corrected and calibrated data, which can then be used to produce more precise and dependable results. An image processing software was utilized to perform radiometric calibration and atmospheric correction in the image pre-processing stage, helping to correct errors present in the raw satellite images.

Image classification is a procedure that assigns pixels into various land cover categories, such as built-up areas, forests, grassland, barren terrain, and other distinguishable classes in the image. The classified data produced is then utilized to generate thematic maps that align with the objectives of a given study. In this research, the software ENVI Classic was employed for image classification. Regions of interest (ROIs) were established for different land cover classes, one set for training and another for accuracy assessment. These ROIs were based on random points created using Google Earth before being established in the ENVI software for image classification. The researchers implemented a Supervised Classification method known as Maximum Likelihood Classification (MLC), and Post Classification-Majority/Minority Analysis to generate land cover maps for the years 1989, 1996, 2017, and 2021. These maps included seven land cover classes: water, barren land, built-up areas, forest, palm, grassland/brush land, and

cropland. A Post-Classification-Majority Analysis was conducted to adjust errant pixels within a single large class where they appear. These maps underwent a correlation analysis to interpret the characterization and changes in land cover in the coastal environment of Banaybanay, Davao Oriental.

Land Cover Classes	Description
Water	All bodies of water like rivers and streams, sea, lakes, reservoir
Barren	Denuded areas, bare soils, bare soils with thin grasses (bare soils is more dominant than grasses), and unpaved roads
Built-up	Residential, commercial, industrial areas, roads and bridges, and all impervious surfaces.
Forest	Includes trees that can be seen in built-up areas, along the roads, parks, and recreational areas. This class also includes sparse vegetation.
Palm	Tract of land containing coconut trees
Grassland/Brushland	Grasses and non-woody plants mixed with shrubs
Cropland	Unplanted cropland planted with crops (rice, corn, etc.)
	Planted with crops (rice, corn, etc.)

**Table 1.** Land cover classification scheme.

**2.4.1 Accuracy assessment.** Accuracy assessment is a crucial aspect to consider in any output generation process. Just as land cover maps are produced, their corresponding accuracies are also evaluated. To assess accuracy, pixel samples were created in the classified image and compared with land class evaluation and reference data. This procedure was carried out using Envi Classic software. Steps from the Envi Classic Menu, specifically Classification > Post Classification > Confusion Matrix Using Ground Truth ROIs, were followed to determine the kappa coefficient and overall accuracy. In addition to the kappa coefficient and overall accuracy, user's and producer's accuracy were also calculated. User's accuracy refers to the percentage of pixels correctly classified in each land cover class according to the reference data. Conversely, producer's accuracy refers to the percentage of pixels correctly classified in each land cover class according to the classified image. By assessing the accuracy of land cover maps using these methods, it allows for an evaluation of the output quality and identification of areas that may need improvement or refinement.

**2.4.2 Land cover change detection.** The study utilized a post-classification comparison change detection method to identify changes in land cover from 1989-2021. This process was carried out using GIS platform. Two classified land cover images were loaded: one from the initial year (1989) and the other from the final year (2021). These two classified raster land cover images were then converted into polygon type using a conversion tool. In the attribute table of the two-classified polygon-type land cover images, the grid code was highlighted, and several features were merged into a single part according to classes using dissolve tools. Intersect tools from geoprocessing were used to identify changes between the initial and final years. New fields named Change and Area\_Change were added in the attribute table. The Field Calculator was used to

determine the land cover class change of the Banaybanay coastal area in the years 1989-2021, with the code [Class\_1989] + " - " + [Class\_2021]. To calculate the total area changes, Calculate Geometry was used. The results were then copied and pasted into a spreadsheet application for further analysis. Change detection analysis of classified images from two different years provides precise, detailed, and quantifiable information about land cover changes, making it a valuable tool for monitoring, management, and policy development in various applications.

## 2.5 Shoreline Change

**2.5.1 Geodatabase creation.** All input data for DSAS were imported and managed within a personal geodatabase, which also served as the storage location for the output files generated by DSAS in the form of feature classes. Both shoreline and baseline feature classes were created as line features and referenced with the same projection, WGS 1984 UTM Zone 51N. Necessary information and requirements were inputted in the shoreline and baseline attribute field.

**2.5.2 Shoreline extraction.** This research made use of four available Landsat satellite images spanning the years 1989 to 2021. The specific years for these images are 1989, 1996, 2017, and 2021. After the images were preprocessed, they were loaded into the ENVI software, and a raster color slice was performed to distinguish land from water.

**2.5.3 Digitization of shoreline.** After performing the raster color slice, shorelines were extracted by digitizing all satellite images of different periods as shapefiles and used as input to the Digital Shoreline Analysis System (DSAS) tool.

**2.5.4 Shoreline data categorization.** The shoreline vectors of different years were merged into a single feature class. It then intersected with the measuring transect that DSAS cast from the baseline. The shoreline feature-class attribute table provide each shoreline vector a date since each reflects a particular point in time. Calculating rates of change requires knowledge about time which the points of intersection offer.

**2.5.5 Baseline creation.** A reference baseline segment was established and placed adjacent to the series of shoreline positions entirely onshore. The baseline is the starting point for all transects cast by the DSAS application. After the shorelines were merged, a buffer was established with a distance of 150 meters. From the baseline, transects intersect each shoreline to create a measurement point, and these measurement points were used to calculate shoreline change statistics.

**2.5.6 Analysis of shoreline change using DSAS.** After baseline creation, transects were cast and established at 500 meters from the baseline and clipped to shoreline extent. Change Statistics tools in the DSAS were then performed. The Net Shoreline Movement (NSM) and Shoreline Change Envelope (SCE) represent the distance, while the Linear Regression Rate (LRR) and End Point Rate (EPR) represent the rate of shoreline change. SCE is the distance between each transect's nearest and furthest shoreline to the baseline. It represents the total change in shoreline movement for all shoreline positions. NSM reports the distance between each transect's earliest and most recent shorelines. It represents the total distance. EPR calculates the distance between the data's oldest and most recent shorelines and divides that distance by the time interval between them.

### 3. RESULTS AND DISCUSSION

#### 3.1 Land Cover Accuracy Assessment

The land cover maps for the years 1989, 1996, 2017, and 2021 were created using Supervised Maximum Likelihood Classification. The results are shown in Figure 4 and Table 2.

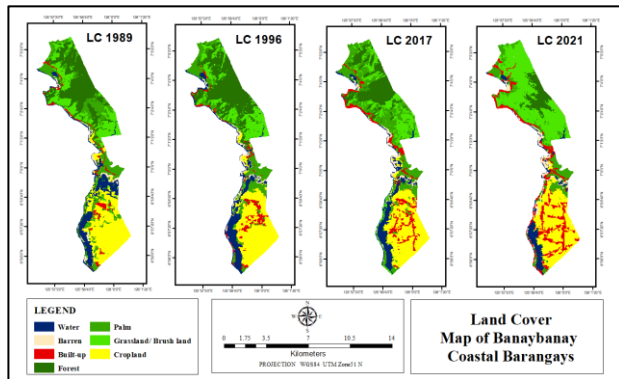


Figure 4. Land cover maps of Banaybanay coastal barangays (1989-2021).

Years	Accuracy Assessment	
	Kappa Coefficient	Overall Accuracy
1989	0.9729	97.9365%
1996	0.9049	92.3810%
2017	0.8831	90.0392%
2021	0.9197	93.1937%

Table 2. Accuracy assessment of land cover maps in the years 1989, 1996, 2017 and 2021.

#### 3.2 Change Detection on Multi-Temporal Land Cover Map

This section provides an overview of the land cover analysis results derived from multi-temporal satellite imagery. The data highlights the extent of each land cover category across four distinct years. The detailed findings are presented in Table 3.

Land Class	Years			
	Area 1989 (ha)	Area 1996 (ha)	Area 2017 (ha)	Area 2021 (ha)
Water	631.32	634.76	541.31	371.76
Barren	127.90	133.13	146.32	213.37
Built-up	190.88	278.67	447.17	735.40
Forest	1,302.47	1,410.89	840.62	381.95
Palm	964.52	846.90	1,398.79	643.17
Grassland/Brushland	905.80	808.02	825.29	1,806.86
Cropland	1,302.63	1,313.04	1,225.45	1,272.59
<b>Class Total</b>	<b>5,425</b>	<b>5,425</b>	<b>5,425</b>	<b>5,425</b>

Table 3. Total areas occupied by each class years.

Between 1989 and 2021, the area covered by water decreased by 259.55 hectares. Barren areas, which include mining zones, saw an increase of 85.47 hectares. Built-up areas expanded by 544.52 hectares. Forest coverage declined by 920.53 hectares, while palm areas reduced by 321.36 hectares. Grassland and brushlands experienced an increase in area from 1989 to 2021, with a total expansion of 901.06 hectares. On the other hand, cropland initially increased in area from 1989 to 1996 but witnessed a significant decrease from 2017 to 2021. Built-up

areas followed a similar pattern to barren lands, indicating an increase in settlements and urbanization due to rapid population growth, as depicted in the graph in Figure 5.

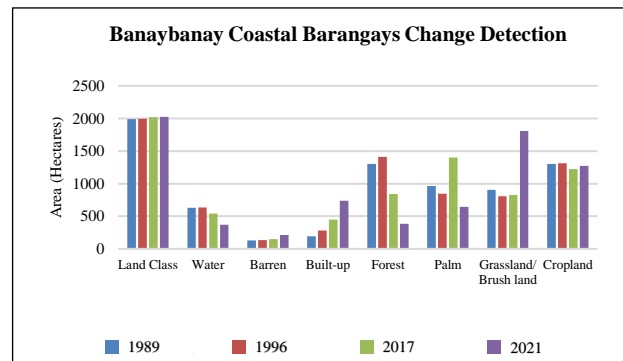


Figure 5. Bar graph showing the change in area of land cover.

Change (1989-2021)	Area Change (ha)
Cropland – Cropland	906.71
Forest – Grassland/ Brushland	809.25
Grassland/ Brushland – Grassland/ Brushland	671.91
Palm – Palm	333.16
Palm – Grassland/ Brushland	311.87
Forest – Forest	284.34
Cropland – Built-up	281.57
Water – Water	259.54
Water – Cropland	152.44
Palm – Built-up	125.77
Others	1,277.16
<b>Total</b>	<b>5,425</b>

Table 4. Total area change from year 1989 to 2021.

Taking into account the initial and final year time targets and the seven land cover classes, the researchers identified 46 potential causes for changes in land cover. As depicted in Figure 6, the primary cause of change is the transition from cropland to cropland and from forest to grassland/brushland, each accounting for 8% of changes, which has a significant impact on the environment. This is followed by grassland/brushland remaining as grassland/brushland (6%), palm remaining as palm (3%), and transitions from palm to grassland/brushland, forest remaining as forest, and cropland to built-up area, each accounting for 3%. Water remaining as water accounts for 2%, while transitions from water to cropland and palm to built-up area each account for 1%. The remaining 62% of changes are attributed to other land cover class changes.

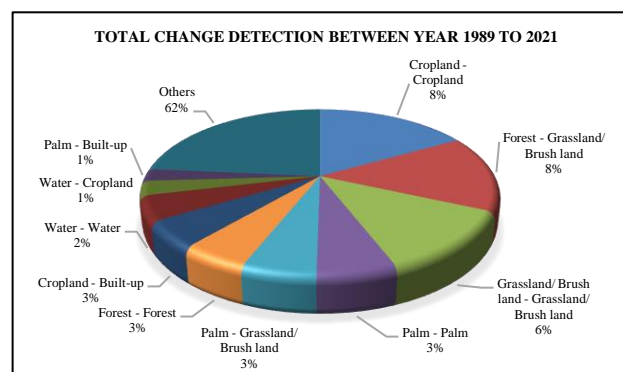


Figure 6. Total change in area of land cover from 1989-2021

### 3.3 Shoreline Change of Banaybanay Coastal Barangays from 1989 to 2021

To analyze the shoreline change of Banaybanay coastal barangays from 1989-2021, three statistical tools from DSAS were employed. These include the Net Shoreline Movement (NSM), End Point Rate (EPR), and Linear Regression Rate (LRR).

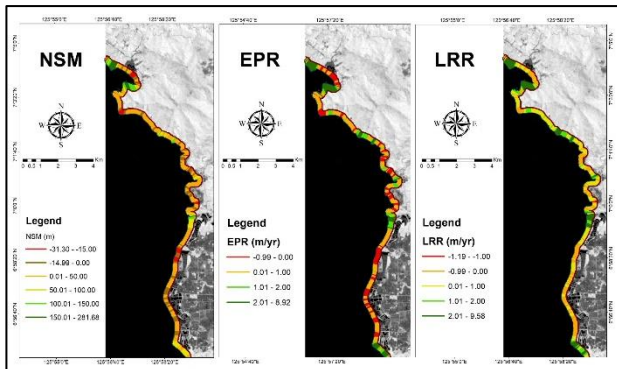


Figure 7. Shoreline change maps based on three statistical tools from DSAS, i.e., NSM, EPR, and LRR.

**3.3.1 Net shoreline movement (NSM).** Figure 7 presents the outcome of the Net Shoreline Movement (NSM), which measures the distance between the oldest and the most recent shorelines for each transect. DSAS cast a total of 497 transects. The statistics reveal that 121 transects have negative values, with -13.1 meters being the greatest distance. Conversely, 376 transects have positive values, with the maximum distance being 281.68 meters. The overall percentage of transects with negative distances is 24.35%, while those with positive distances account for 75.65%.

Net Shoreline Movement (NSM)			
	Total Number	Overall Percentage	Maximum Value (m/yr)
Erosional Transects	121	24.35%	-13.1
Accretional Transects	376	75.65%	281.68

Table 5. Statistics of shoreline change derived from NSM.

**3.3.2 End point rate (EPR).** As shown in Figure 7, it displays the results of the End Point Rate (EPR), which is calculated by dividing the distance between the oldest and youngest shorelines (NSM) by the time elapsed between them, in this case, 32 years. The rate is measured in meters per year. Erosion and accretion levels were divided into seven categories: very high erosion ( $> -2$ ), high erosion ( $> -1$  and  $< -2$ ), moderate erosion ( $> 0$  and  $< -1$ ), stable (0), moderate accretion ( $> 0$  and  $< +1$ ), high accretion ( $> +1$  and  $< +2$ ), and very high accretion ( $> +2$  meters/year). DSAS cast a total of 497 transects. The statistics show that 121 transects are erosional, while 376 are accretional. The maximum value of erosion, classified as moderate erosion, is reported as -0.19 m/year. In contrast, the maximum value of accretion, classified as very high accretion, is reported as 8.92 m/year. The overall percentage of erosional transects is calculated as 24.35%, while the overall percentage of accretional transects is calculated as 75.65%.

Category	Rate of Shore Change (m/yr)	Shoreline Classification
1	$> -2$	Very high erosion
2	$> -1$ and $< -2$	High erosion
3	$> 0$ and $< -1$	Moderate erosion
4	0	Stable
5	$> 0$ and $< +1$	Moderate accretion
6	$> +1$ and $< +2$	High accretion
7	$> +2$	Very high accretion

Table 6. Category of shoreline classification (Nassar et al., 2018)

End Point Rate (EPR)				
	Total Number	Overall Percentage	Max. Value (m/yr)	Shore Classification
Erosional Transects	121	24.35%	-0.99	Moderate Erosion
Accretional Transects	376	75.65%	8.92	Very high accretion

Table 7. Statistics of shoreline change derived from EPR.

**3.3.3 Linear regression rate (LRR).** Figure 7 presents the outcome of the Linear Regression Rate (LRR), which is calculated by fitting a least-squares regression line to all shoreline points for each transect. The rate is measured in meters per year. Erosion and accretion levels were divided into seven categories: very high erosion ( $> -2$ ), moderate erosion ( $> -1$  and  $< -2$ ), moderate erosion ( $> 0$  and  $< -1$ ), stable (0), moderate accretion ( $> 0$  and  $< +1$ ), high accretion ( $> +1$  and  $< +2$ ), and very high accretion ( $> +2$  meters/year). DSAS cast a total of 497 transects. The statistics show that 169 transects are erosional, with a maximum erosional value of -1.19 m/year, categorized as high erosion. Conversely, there are 327 accretional transects, with a maximum value of 9.58 m/year, classified as very high accretion. The overall percentage of erosional transects is calculated as 34.07%, while the overall percentage of accretional transects is calculated as 65.93%.

Linear Regression Rate (LRR)				
	Total Number	Overall Percentage	Max. Value (m/yr)	Shore Classification
Erosional Transects	169	34.07%	-1.19	High Erosion
Accretional Transects	327	65.93%	9.58	Very high accretion

Table 8. Statistics of shoreline change derived from LRR.

### 3.4 Shoreline Change Determination in Two (2) Coastal Barangays

Additional shoreline change processing was carried out by the researchers in Barangay Puntalino and Pintatagan, areas experiencing very high accretion, to gather more data. The highest-resolution images from 2009, 2014, 2017, and 2019 were obtained from Google Earth and geo-referenced. A color slice of the raster was then performed to distinguish between land and water. The shorelines were digitized, and the same procedure was repeated.

**3.4.1 Net shoreline movement (NSM) calculation based on Google Earth image.** Figure 8 presents the outcome of the Net Shoreline Movement (NSM). DSAS cast a total of 134 transects. The statistics reveal that ten transects have negative values, with -10.65 meters being the greatest distance.

Conversely, 124 transects have positive values, with the maximum distance being 164.95 meters. The overall percentage of transects with negative distances is 7.46%, while those with positive distances account for 92.54%.

Net Shoreline Movement (NSM)			
	Total Number	Overall Percentage	Maximum Value (m/yr)
Erosional Transects	10	7.46%	-10.65
Accretional Transects	124	92.54%	164.95

**Table 9.** Statistics of shoreline change for NSM based on Google Earth image.

**3.4.2 End point rate (EPR) calculation based on Google Earth image.** Figure 8 presents the results of the End Point Rate (EPR) derived from Google Earth images. The rate is measured in meters per year. Erosion and accretion levels were divided into seven categories: Very high erosion (> -2), High erosion (> -1 and < -2), Moderate erosion (> 0 and < -1), Stable (0), Moderate accretion (> 0 and < +1), High accretion (> +1 and < +2), and Very high erosion (> +2 meters/year). DSAS cast a total of 134 transects. The statistics show that ten transects are erosional, while 124 are accretional. The maximum value of erosion, classified as moderate erosion, is reported as -0.9 m/year. In contrast, the maximum value of accretion, classified as high erosion, is reported as 13.97 m/year. The overall percentage of erosional transects is calculated as 7.46%, while the overall percentage of accretional transects is calculated as 92.54%.

End Point Rate (EPR)				
	Total Number	Overall Percentage	Max. Value (m/yr)	Shore Classification
Erosional Transects	10	7.46%	-0.9	Moderate Erosion
Accretional Transects	124	92.54%	13.97	Very high accretion

**Table 10.** Statistics of shoreline change for EPR based on Google Earth image.

**3.4.3 Linear regression rate (LRR) calculation based on Google Earth image.** Figure 8 shows the result of the Linear Regression Rate (LRR) using google earth images. The rate was measured as meter/year. The level of erosion and accretion were classified into seven categories as follows: Very high erosion with > -2, Moderate erosion with > -1 and < -2, Moderate erosion with > 0 and < -1, Stable with 0, Moderate accretion with > 0 and < +1, High accretion with > +1 and < +2, and Very high erosion with > +2 m/yr. There is a total of 134 transects that the DSAS cast. The results of the statistics reported 18 erosional transects with a maximum erosional value of -0.96 m/yr, categorized as high erosion. On the other hand, there are 116 erosional transects with a maximum value of 15.97 m/yr, classified as very high erosion. The overall percent of all erosional transects was calculated as 13.43%, while the percentage of all accretional transects was calculated as 86.57%.

Linear Regression Rate (LRR)				
	Total Number	Overall Percentage	Max. Value (m/yr)	Shore Classification
Erosional	18	13.43%	-0.96	Moderate

Transects				Erosion
Accretional Transects	116	86.57%	15.97	Very high accretion

**Table 11.** Statistics of shoreline change for LRR based on Google Earth image.

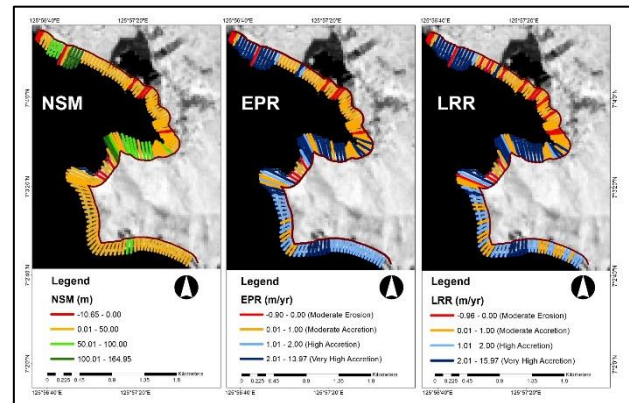


**Figure 8.** Shoreline change maps based on Google Earth image (NSM, EPR, LRR).

### 3.5 Future Projection of the Shoreline

The process of shoreline forecasting generates predictions for the next 10 and 20 years based on the input shoreline data. This is achieved by merging observed shoreline positions with positions derived from a model. The DSAS Kalman filter approach, which is initialized with the linear regression rate calculated by DSAS, estimates the shoreline position and change rate for every tenth of a year. Given that the Linear Regression Rate (LRR) calculation indicates a higher number of accretional transects, it is anticipated that the forecasted position of the shoreline for 2031 and 2041 will likely be in a seaward position. This corresponds to accretion in certain areas.

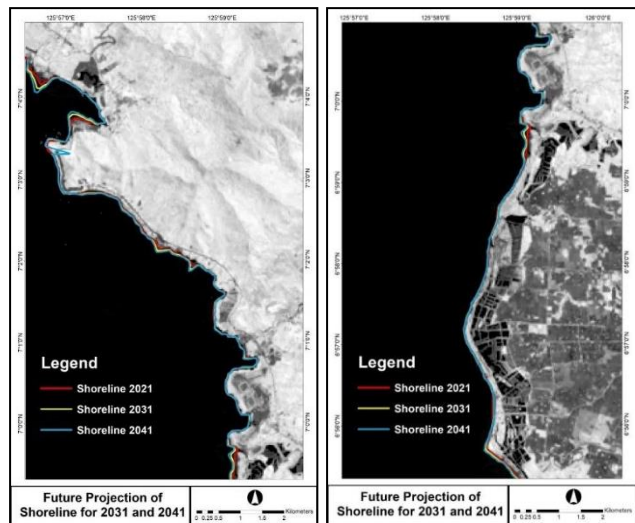


**Figure 9.** Future projection of the shoreline for the next 10 and 20 years.

### 3.6 Land Cover and Shoreline Change Characterization

For the characterization of land cover and shoreline change, the transects that were cast were overlaid on the 2021 land cover map. This was done to identify the land cover classes where the transects were cast, along with their corresponding categories of shoreline classification.

Shoreline Classification	Land Cover Change	Number of Transects
High Erosion	Barren – Water	2
	Grassland/Brushland – Water	1
Moderate Erosion	Grassland/Brushland – Water	66
	Barren – Water	61
	Palm – Water	25
	Built-up – Water	25
Moderate Accretion	Water – Built-up	94
	Water – Barren	60
	Barren – Built-up	31
	Barren – Barren	24
	Grassland/Brushland – Built-up	3
High Accretion	Water – Built-up	29
	Barren – Barren	15
	Built-up – Built-up	4
Very High Accretion	Water – Built-up	44
	Barren – Built-up	10
	Water – Barren	7

**Table 12.** Land cover change with its number of transects.

#### 4. CONCLUSION

The extraction and analysis of shoreline change is a crucial task with applications in various fields, including setback planning, hazard zoning, erosion-accretion studies, regional sediment budgets, and conceptual or predictive modeling of coastal morphodynamics.

In this study, the researchers used available Landsat satellite images from 1989, 1996, 2017, and 2021 to determine the land cover change in the coastal barangays of Banaybanay and the shoreline change in the area. The findings revealed a rapid change in land cover from 1989 to 2021. This suggests that an increase in mining activities, human activities, and urbanization can lead to a rapid change in land cover and shoreline. The analysis of multiple time-series satellite images can enable continuous monitoring of mining and human activities in the areas under study. Moreover, it can potentially predict future trends in land use and land cover dynamics over the studied area, specifically the coastal barangay of Banaybanay, Davao Oriental.

To gain further insights into areas experiencing very high accretion, the researchers utilized the highest-resolution images available on Google Earth from 2009, 2014, 2017, and 2021. The Digital Shoreline Analysis System (DSAS), an extension of ArcGIS, was employed to calculate shoreline change using the Net Shoreline Movement (NSM), End Point Rate (EPR), and Linear Regression Rate (LRR). These measurements reported changes in distance (in meters) and rate of change (in meters/year). According to the shoreline change statistics, NSM reported a maximum negative distance of -31.30 meters with 24.35% of all transects having negative distances and a maximum positive distance of 281.68 meters with 75.65% of all transects having positive distances. EPR results showed a maximum erosion value of -0.99 m/yr (classified as moderate erosion) with 24.35% of all transects being erosional, and a maximum accretion value of 8.92 m/yr (classified as very high accretion) with 75.65% of all transects being accretional. LRR results reported a maximum erosion value of -1.19 m/yr (classified as high erosion) with 43.07% of all transects being erosional, and a maximum accretion value of 9.58 m/yr

(classified as very high accretion) with 65.93% of all transects being accretional. The overall results indicate that the coastal areas of Banaybanay, Davao Oriental, are experiencing accretion due to urbanization and growth development.

For the characterization of land cover and shoreline changes, it was found that the land cover changes leading to high erosion correspond to barren-water and grassland/brushland-water transitions. Moderate erosion corresponds to transitions from grassland/brushland-water, barren-water, palm-water, and built-up-water. Moderate accretion corresponds to transitions from water-built-up, water-barren, barren-built-up, barren-barren, and grassland/brushland-built-up. High accretion corresponds to transitions from water-built-up, barren-barren, and built-up-built-up. Very high accretion corresponds to transitions from water-built-up, barren-built-up, and water-barren. This characterization was conducted to identify the land cover classes within the coastal areas that may be prone or vulnerable to shoreline change in the coming years (both erosion and accretion).

#### REFERENCES

- Azatuhi, H., Garegin, T., Vahagn, M., Shushanik, A., Andrey, M., Alexander, K., 2019: Lake sevan shoreline change assessment using multi-temporal landsat images. *Geogr. Environ. Sustain.*, vol. 12, no. 4, pp. 212–229. doi.org/10.24057/2071-9388-2019-46.
- Islam, M. S., Uddin, M. A., Hossain, M. A., 2021: Assessing the dynamics of land cover and shoreline changes of Nijhum Dwip (Island) of Bangladesh using remote sensing and GIS techniques. *Reg. Stud. Mar. Sci.*, vol. 41, p. 101578. doi.org/10.1016/j.rsma.2020.101578.
- Makota, V., Sallema, R., Mahika, C., 2004: Monitoring shoreline change using remote sensing and GIS: A case study of Kunduchi Area, Tanzania. *West. Indian Ocean J. Mar. Sci.*, vol. 3, no. 1, pp. 1–10.
- Nassar, K., Mahmod, W. E., Fath, H., Masria, A., Nadaoka, K., Negm, A., 2018: Shoreline change detection using DSAS technique: Case of North Sinaicoast, Egypt. *Marine Georesources & Geotechnology*. doi.org/10.1080/1064119X.2018.1448912.
- Tamassoki, E., Amiri, H., Soleymani, Z., 2014: Monitoring of shoreline changes using remote sensing (case study: Coastal city of Bandar Abbas). *IOP Conf. Ser. Earth Environ. Sci.*, vol. 20, no. 1. doi.org/10.1088/1755-1315/20/1/012023.
- Thao, P. T. P., Duan, H. D., To, D. V., 2008: Integrated remote sensing and GIS for calculating shoreline change in Phan-Thiet coastal area. *Int. Symp. Geoinformatics Spat. Infrastruct. Dev. Earth Allied Sci.*, pp. 1–6.
- Zonkouan, B. R. V., Bachri, I., Beda, A. H. J., N’guessan, K. A. M., 2022: Monitoring spatial and temporal scales of shoreline changes in lahou-kpanda (Southern ivory coast) using landsat data series (tm, etm+ and oli). *Geomatics Environ. Eng.*, vol. 16, no. 1, pp. 145–158. doi.org/10.7494/geom.2022.16.1.145.